Articles

Indenyl Rhenium Alkyne Complexes: CO Substitution via Alkyne-Assisted Ring Slippage and CO-Catalyzed Phosphine Substitution

Charles P. Casey,* Thomas E. Vos, John T. Brady, and Randy K. Hayashi

Department of Chemistry, University of Wisconsin−Madison, Madison, Wisconsin 53706

Received October 23, 2002

CO substitution of the indenyl alkyne complex (η^5-C_9H_7)$(CO)_2$Re(η^2-MeC≡CMe) (**3**) to form (η^5-C_9H_7)$Re(CO)_3$ (**8**) is much faster than that of either the indenyl alkene complex (η^5-C_9H_7)$(CO)_2$Re(η^2-*cis*-MeHC═CHMe) (**2**) or the cyclopentadienyl alkyne complex (η^5-C_5H_5)$(CO)_2$Re(η^2-MeC≡CMe) (**5**). The acceleration of the reaction of **3** with CO is proposed to involve cooperativity between slippage of the indenyl ring from an η^5 6e-donor to an η^3 4e-donor and shifting of the alkyne ligand from a 2e- to a 4e-donor as CO associates with the rhenium complex. The rate of reaction of **3** with CO showed a linear dependence on CO pressure between 1 and 10 atm, consistent with CO-promoted indenyl ring slippage. At very high CO pressure, **3** is rapidly converted to (η^1-C_9H_7)$(CO)_4$Re(η^2-MeC≡CMe) (**12**). Upon release of CO pressure, **12** reverts to a 12:1 mixture of starting material **3** and CO substitution product **8** at a rate that is inversely dependent on CO pressure. When the reaction of ^{13}CO with **3** was carried to about 50% conversion, extensive labeling of starting material **3** and product **8** was observed. The distribution of label in **3** and **8** requires largely stereospecific ^{13}CO addition to form mainly one isomer of an η^3-indenyl intermediate (η^3-C_9H_7)$(CO)_2$(^{13}-CO)Re(η^2-MeC≡CMe) (**B-(^{13}CO)$_1$**) along with a minor amount of a second stereoisomer of **B-(^{13}CO)$_1$** and the involvement of double-labeled η^1-indenyl complex **12-(^{13}CO)$_2$**. The reaction of **3** with PPh_3 to form the phosphine complex (η^5-C_9H_7)$(CO)_2$Re(PPh_3) (**9**) is catalyzed by ^{13}CO. The observation of ^{13}CO in **9** is consistent with the proposal that **9** is formed by trapping a reactive intermediate in the CO substitution reaction of **3**.

In connection with our search for heterobimetallic dihydrides that might serve as powerful new reducing agents, we synthesized the heterobimetallic dihydride $Cp(CO)_2Re(\mu$-H)Pt(H)$(PPh_3)_2$ (**1**) by reaction of Cp-$(CO)_2ReH_2$ with $(CH_2═CH_2)Pt(PPh_3)_2$.[1,2] We were delighted to find that **1** reduced alkynes to produce high yields of rhenium alkene complexes and platinum alkyne complexes (Scheme 1). We also found that Pt(0) complexes catalyzed the reaction of *trans*-$Cp(CO)_2ReH_2$ with alkynes to give rhenium alkene complexes. Unfortunately, because of the high stability of rhenium alkene complexes, these reactions were stoichiometric in rhenium.

Since the stability of these $Cp(CO)_2Re$(alkene) complexes toward substitution interfered with the development of a catalytic process, we began investigations of related (η^5-indenyl)$(CO)_2$Re(alkene) complexes which we anticipated would undergo alkene exchange more rapidly. Substitution of the indenyl ligand for the cyclopentadienyl ligand in metal complexes often leads to

Scheme 1

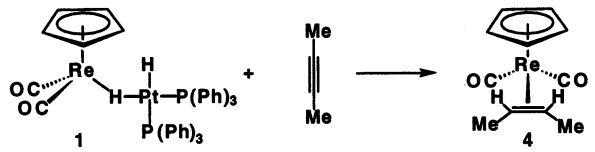

increased rates of substitution, usually referred to as the "indenyl effect". Basolo found that the rate of PPh_3 substitution on (η^5-C_9H_7)$Rh(CO)_2$ was 10^8 times faster than the analogous Cp system (Scheme 2).[3] The rate dependence on phosphine concentration indicated that the reaction proceeded via an associative process. A mechanism involving simultaneous addition of PPh_3 to rhodium and indenyl ring slippage from η^5 to η^3 coordination was proposed. Mawby showed that the indenyl ligand can also increase the rates of substitution in dissociative reactions. The reaction of (η^5-C_9H_7)Fe-$(CO)_2$I with $P(OEt)_3$ proceeded 575 times faster than the analogous Cp system.[4] Initially the indenyl effect was explained in terms of enhanced stability of the η^3-indenyl due to increased aromaticity of the six-mem-

(1) Casey, C. P.; Rutter, E. W., Jr.; Haller, K. J. *J. Am. Chem. Soc.* **1987**, *109*, 6886.
(2) (a) Casey, C. P.; Rutter, E. W., Jr. *J. Am. Chem. Soc.* **1989**, *111*, 8917. (b) Casey, C. P.; Wang, Y.; Tanke, R. S.; Hazin, P. N.; Rutter, E. W., Jr. *New J. Chem.* **1994**, *18*, 43.

(3) Rerek, M. E.; Basolo, F. *J. Am. Chem. Soc.* **1984**, *106*, 5908.
(4) Jones, D. J.; Mawby, R. J. *Inorg. Chim. Acta* **1972**, *6*, 157.

10.1021/om020884q CCC: $25.00
Publication on Web 02/08/2003

Scheme 2

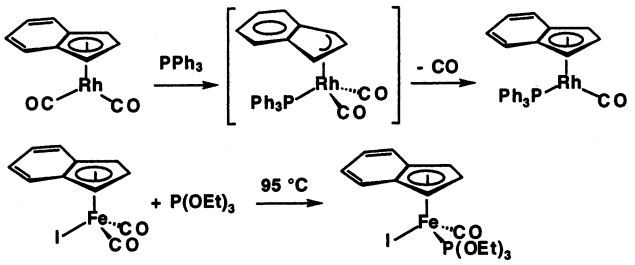

bered ring upon slippage. More recently, it has also been noted that the η^5-indenyl ligand is bound to the metal less strongly than an η^5-Cp ligand due to weaker bonding to the carbons shared with the aryl ring, and it has been suggested that η^5-indenyl binding might be better described as "$\eta^3 + \eta^2$" binding.[5]

Here we report the synthesis of $(\eta^5\text{-}C_9H_7)(CO)_2Re(\eta^2\text{-}cis\text{-}MeHC{=}CHMe)$ (**2**) and $(\eta^5\text{-}C_9H_7)(CO)_2Re(\eta^2\text{-}MeC{\equiv}CMe)$ (**3**) and their substitution reactions. In the course of studying these substitution reactions, we uncovered a unique cooperative interaction between an indenyl ligand and an alkyne ligand that leads to unusually fast processes. The ability of the alkyne to function as either a 2e- or a 4e-donor apparently stabilizes the transition state for CO-promoted η^5- to η^3-indenyl ring slippage. Further evidence for ring slippage was obtained by the observation of the η^1-intermediate $(\eta^1\text{-}C_9H_7)(CO)_4Re(\eta^2\text{-}MeC{\equiv}CMe)$ (**12**) at very high CO pressure. We have also found that CO catalyzes the substitution of PPh_3 for butyne in **3**. This is the *first example of a CO-catalyzed phosphine substitution reaction*. While it is now clear that the indenyl system will not provide sufficient acceleration of alkene dissociation to be useful in heterobimetallic catalytic systems, the results reported here provide new insight into the mechanism of substitution reactions that are often of crucial importance in catalytic processes.

Results

One important obstacle to developing alkyne hydrogenation catalysts based on the chemistry of $Cp(CO)_2Re(\mu\text{-}H)Pt(H)(PPh_3)_2$ is the high thermal stability of the resulting rhenium alkene products. The $Cp(CO)_2Re$(alkene) complexes do not release alkene until heated above 140 °C. For example, treatment of a C_6D_6 solution of $Cp(CO)_2Re(\eta^2\text{-}cis\text{-}MeHC{=}CHMe)$ (**4**) with excess 2-butyne at 140 °C for 33 h led to only 31% conversion of **4** to a mixture of $Cp(CO)_2Re(\eta^2\text{-}MeC{\equiv}CMe)$ (**5**) (16%) and unidentified products (15%). In search of more labile alkene complexes, we began investigations of the indenyl complex $(\eta^5\text{-}C_9H_7)(CO)_2Re(\eta^2\text{-}cis\text{-}MeHC{=}CHMe)$ (**2**) as a possibly more reactive alternative.

Synthesis of $(\eta^5\text{-}C_9H_7)(CO)_2Re(\eta^2\text{-}cis\text{-}MeHC{=}CHMe)$ (2) and $(\eta^5\text{-}C_9H_7)(CO)_2Re(\eta^2\text{-}MeC{\equiv}CMe)$ (3). The indenyl rhenium THF complex $(\eta^5\text{-}C_9H_7)Re(CO)_2$(THF) (**7**) obtained by photolysis of $(\eta^5\text{-}C_9H_7)Re(CO)_3$ (**8**) proved to be a valuable intermediate for the synthesis of alkene, alkyne, and phosphine complexes. A yellow THF solution of **7** reacted with excess *cis*-2-butene at room temperature over several hours to form a yellow-orange solution of $(\eta^5\text{-}C_9H_7)(CO)_2Re(\eta^2\text{-}cis\text{-}MeHC{=}CHMe)$ (**2**), which was isolated as a yellow-orange crystalline solid (43%). The structure of **2** was established spectroscopically and confirmed by X-ray crystallography (Figure 1). The indenyl ligand is bound with three shorter distances to carbon [Re−C(8), 2.267(7) Å; Re−C(9), 2.283(8) Å; Re−C(10), 2.302(8) Å] and two longer distances to the carbons shared with the aryl ring [Re−C(11), 2.382(7) Å; Re−C(7), 2.393(8) Å]; the folding angle Ω of the indenyl ligand is 7(1)°. The angle between the C=C bond of coordinated 2-butene and the indenyl ring is 22°.

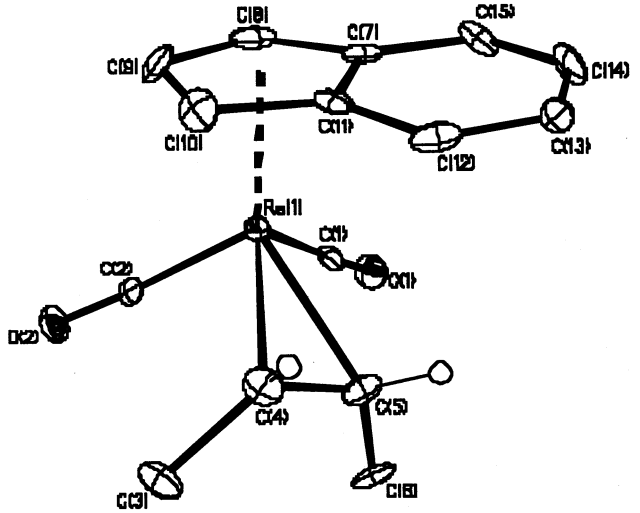

Figure 1. X-ray crystal structure of $(\eta^5\text{-}C_9H_7)(CO)_2Re(\eta^2\text{-}cis\text{-}MeHC{=}CHMe)$ (**2**).

Scheme 3

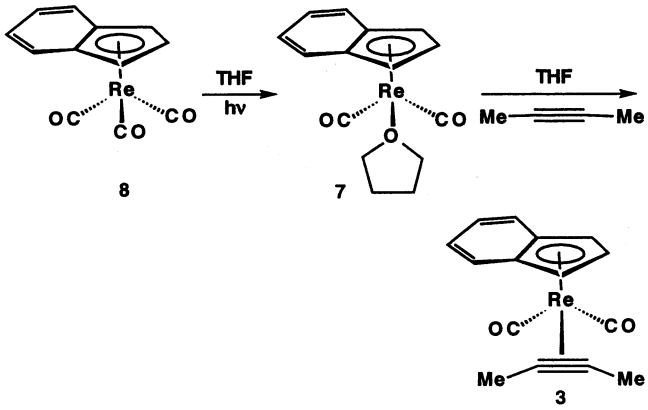

The indenyl rhenium THF complex **7** reacted with excess 2-butyne in THF over 1 h to produce the alkyne complex $(\eta^5\text{-}C_9H_7)(CO)_2Re(\eta^2\text{-}MeC{\equiv}CMe)$ (**3**), which was isolated as an orange solid (35%) (Scheme 3). The structure of **3** was established spectroscopically and confirmed by X-ray crystallography (Figure 2). As in the case of alkene complex **2**, the indenyl ligand of **3** is bound with three shorter distances to carbon [Re−C(8b), 2.229(13) Å; Re−C(9b), 2.286(13) Å; Re−C(10b), 2.320-(13) Å] and two longer distances to the carbons shared with the aryl ring [Re−C(11b), 2.409(13) Å; Re−C(7b), 2.424(13) Å]; the folding angle Ω of the indenyl ligand is 2(2)°. The angle between the C≡C bond of coordinated 2-butyne and the indenyl ring is 6°. The methyl groups of 2-butyne are bent away from Re by 27°.

(5) (a) Calhorda, M. J.; Veiros, L. F. *Coord. Chem. Rev.* **1999**, *186*, 37. (b) Veiros, L. F. *Organometallics* **2000**, *19*, 3127. (c) Calhorda, M. J.; Romão, C. C.; Veiros, L. F. *Chem. Eur. J.* **2002**, *8*, 868. (d) Kubas, G. J.; Kiss, G.; Hoff, C. D. *Organometallics* **1991**, *10*, 2870.

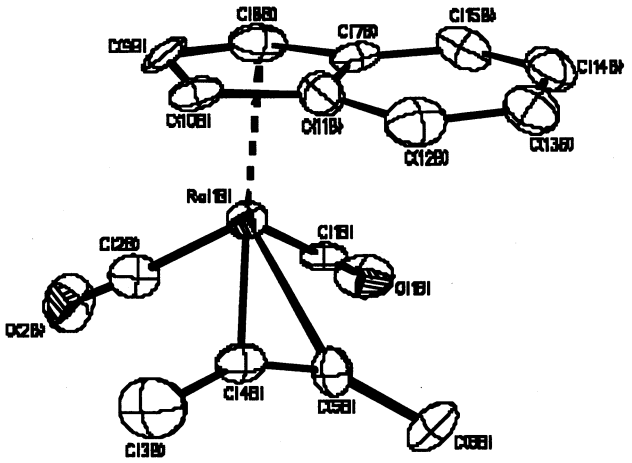

Figure 2. X-ray crystal structure of (η^5-C_9H_7)$(CO)_2$Re(η^2-MeC≡CMe) (**3**).

2-Butyne Exchange with (η^5-C_9H_7)$(CO)_2$Re(η^2-*cis*-MeHC=CHMe) (2). The indenyl alkene complex (η^5-C_9H_7)$(CO)_2$Re(η^2-*cis*-MeHC=CHMe) (**2**) proved to have high thermal stability like its Cp analogue **4**. Reaction of excess 2-butyne with alkene complex **2** in C_6D_6 at 140 °C led to the formation of the alkyne complex (η^5-C_9H_7)$(CO)_2$Re(η^2-MeC≡CMe) (**3**) (maximum 29% yield) along with decomposition products. The disappearance of alkene complex **2** at 140 °C was monitored by ^{1}H NMR spectroscopy at 25 °C. The rate of disappearance of **2** was first order in rhenium to over 3 half-lives ($k_{obs} = 4.1 \times 10^{-6}$ s^{-1}, $t_{1/2} = 2$ days, $\Delta G^{\ddagger}$ at 140 °C = 34.6 kcal mol^{-1}). The reverse reaction where alkyne complex **3** reacted with excess *cis*-2-butene proceeded at lower temperature (85 °C) ($k_{obs} = 5.0 \times 10^{-7}$ s^{-1}, $t_{1/2} = 16$ days, $\Delta G^{\ddagger}$ at 85 °C = 31.4 kcal mol^{-1}) and cleanly produced 2-butene complex **2** (only ~5% uncharacterized decomposition products). The activation barrier for substitution of alkyne complex **3** was 3.2 kcal mol^{-1} lower than that of alkene complex **2**. The slow rate of alkene−alkyne exchange of these indenyl complexes indicates that use of an indenyl analogue of alkyne hydrogenation catalyst $Cp(CO)_2$Re(μ-H)Pt(H)-$(PPh_3)_2$ (**1**) would not provide the improvement that we had hoped for.

Attempted CO Substitution Reactions of C_5H_5-$(CO)_2$Re(η^2-*cis*-MeHC=CHMe) (4) and $C_5H_5(CO)_2$Re-(η^2-MeC=CMe) (5). To establish a baseline of reactivity for comparison with reactions of indenyl complexes, we first investigated the reactions of $C_5H_5(CO)_2$Re(η^2-*cis*-MeHC=CHMe) (**4**) and $C_5H_5(CO)_2$Re(η^2-MeC≡CMe) (**5**) with CO. When a C_6H_6 solution of Cp alkene complex **4** was heated at 80 °C under 4 atm of CO, no reaction was observed after 3 days ($\Delta G^{\ddagger}$ at 80 °C > 31 kcal mol^{-1}). This is consistent with the high thermal stability of **4** observed in its slow reaction with 2-butyne at 140 °C.

The reaction of CO with $C_5H_5(CO)_2$Re(η^2-MeC≡CMe) (**5**) was also very slow. Treatment of a C_6D_6 solution of **5** with 4 atm of ^{13}CO at 25 °C led to only 3.3% conversion of **5** to C_5H_5Re$(CO)_3$ (**6**) after 24 days ($\Delta G^{\ddagger}$ at 25 °C > 28 kcal mol^{-1}). Treatment of a C_6D_6 solution of $C_5H_5(CO)_2$Re(η^2-MeC≡CMe) (**5**) (containing 0.35 equiv of 2,6-dimethylpyridine to prevent the acid-catalyzed isomerization to the allene complex $C_5H_5(CO)_2$Re(η^2-2,3-MeCH=C=CH$_2$))[6] at 80 °C under 2.3 atm ^{13}CO for 7 h led to complete disappearance of alkyne complex **5**, 16% conversion to C_5H_5Re$(CO)_3$ (**6**), and decomposition to uncharacterized black solids. Thus, the reactions of both **4** and **5** with CO proved to be so slow that quantitative rate measurements were not readily determined.

Scheme 4

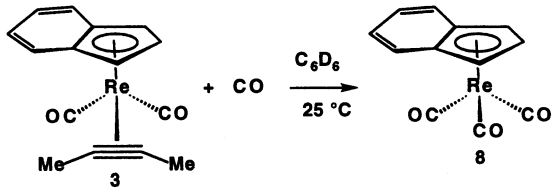

Reaction of CO with (η^5-C_9H_7)$(CO)_2$Re(η^2-*cis*-MeHC=CHMe) (2) and (η^5-C_9H_7)$(CO)_2$Re(η^2-MeC≡CMe) (3). The reactions of indenyl alkene and alkyne complexes **2** and **3** with CO were much faster than those of the corresponding Cp complexes. The conversion of **2** to (η^5-C_9H_7)Re$(CO)_3$ (**8**) occurred over several days in C_6H_6 solution at 25 °C under 4.1 atm CO. The reaction of **2** with CO at 25 °C was monitored by IR analysis of 0.3 mL aliquots removed from a pressure reaction vessel. The rate of disappearance of **2** was first order in rhenium through three half-lives (k_{obs} of 6.4×10^{-6} s^{-1}, $t_{1/2} = 30$ h, $\Delta G^{\ddagger}$ at 25 °C ≈ 24.5 kcal mol^{-1}). The carbonylation of indenyl alkene complex **2** was much faster than the carbonylation of Cp alkene complex **4**. The indenyl ligand accelerated the rate of CO substitution but was ineffective in promoting reaction of **2** with 2-butyne. CO reacted with **2** under very mild conditions (4.1 atm CO, 25 °C), but reaction of **2** with 2-butyne required heating to 140 °C for days.

The reaction of indenyl *alkyne* complex **3** with CO was 27 times faster than the reaction of indenyl *alkene* complex **2** with CO. When a C_6H_6 solution of **3** under 4.1 atm CO at 25 °C was rapidly stirred, formation of (η^5-C_9H_7)Re$(CO)_3$ (**8**) occurred over several hours (Scheme 4). The rate of disappearance of the carbonyl bands of **3** at 1943 and 1869 cm^{-1} was first order in rhenium through 3 half-lives (k_{obs} of 1.8×10^{-4} s^{-1}, $t_{1/2} = 1.1$ h).

Examination of the rates of reaction of CO with the indenyl and Cp complexes of alkenes and alkynes indicates that the special combination of indenyl and alkyne ligands leads to an unusually fast reaction. This apparent cooperativity led us to investigate the reaction of **3** with CO in greater detail in an attempt to understand how the indenyl and alkyne ligands work together to accelerate substitution reactions.

Pressure Dependence of the CO Substitution of 3. The rate of formation of **8** from **3** in the presence of CO was measured over a wide range of CO pressures (1−120 atm) (Table 1, Figure 3). The rate of CO substitution in the pressure range of 1−10 atm CO was measured by following the appearance of the IR bands of **8** and the disappearance of the IR bands of **3**. To avoid depleting the concentration of CO in solution, the solutions were rapidly stirred and the concentration of rhenium complexes (4−8 mM) was kept low compared with the concentration of CO in solution (8−30 mM).[7]

The rate of CO substitution of **3** was also followed by NMR in the pressure range 2−5 atm. While NMR

(6) Casey, C. P.; Brady, J. T. *Organometallics* **1998**, *17*, 4620−4629.

Table 1. CO Pressure Dependence on the Rate of Formation of (η^5-C_9H_7)Re(CO)$_3$ (8) at 25 °C from (η^5-C_9H_7)(CO)$_2$Re(η^2-MeC≡CMe) (3)

CO (atm)	[CO] (mM)	[Re] (mM)	$k_{obs} \times 10^4$ (s^{-1})	$t_{1/2}$ (min)
1.1[a]	8	8	0.53	217
2.1[a]	15	10	1.1	103
3.0[a]	21	5	1.8	63
4.1[a]	29	8	1.8	66
2.2[b]	15	58	0.60	193
3.0[b]	20	55	1.3	90
3.9[b]	26	46	1.5	80
4.3[b]	28	66	1.7	66
4.2[b]	28	57	2.4	49
5.3[b]	36	41	2.6	45
10.9[c]	76	2	4.8	24
17.6[c]	123	3	7.4	16
27.6[c]	193	2	8.2	14
37.9[c]	265	2	8.1	14
40.8[c]	285	5	8.3	14
100[c]	699	2	8.0	14
10.2[d]	71	5	4.2	28
20.4[d]	143	5	8.0	14
34.0[d]	238	5	9.7	12
68.0[d]	475	6	9.5	12
76.5[d]	535	4	8.7	13
102.0[d]	713	4	6.9	16
120.0[d]	839	4	5.6	19

[a] Rate measured by IR spectroscopy after release of CO pressure. [b] Rate measured by in situ ^{1}H NMR spectroscopy. [c] Reaction run in high-pressure reaction vessel and mixture analyzed by ^{1}H NMR spectroscopy after release of pressure. [d] Rate measured by in situ IR spectroscopy.

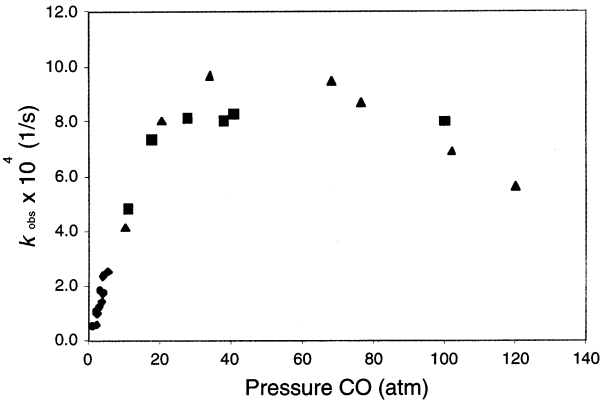

Figure 3. CO pressure dependence of the rate of formation of (η^5-C_9H_7)Re(CO)$_3$ (**8**) from (η^5-C_9H_7)(CO)$_2$Re(η^2-MeC≡CMe) (**3**). ● = k_{obs} from IR spectroscopy after release of CO pressure. ◆ = k_{obs} from in situ ^{1}H NMR spectroscopy. ■ = k_{obs} from reaction run in high-pressure reaction vessel and product mixture analyzed by ^{1}H NMR spectroscopy after release of pressure. ▲ = k_{obs} from in situ IR spectroscopy.

allowed in situ monitoring, the limited gas/liquid surface area in NMR tubes limits the rate of gas dissolution and can result in mass transfer limited rates. Despite this problem, the rates measured by the two methods are in fair agreement with one another. The rate of appearance of **8** measured by NMR spectroscopy and IR spectroscopy showed a linear dependence on CO pressure over the range from 1 to 10 atm. At higher pressures of CO (>10−120 atm), we measured the rate

Scheme 5

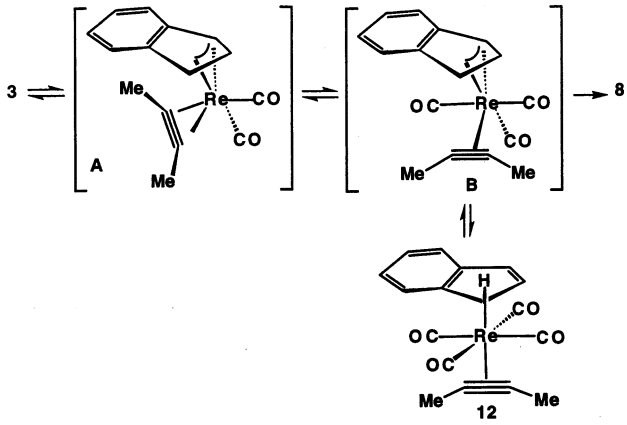

of appearance of **8** by two different methods. In the first method, we determined the rate of appearance of **8** by two-point kinetic analysis. We added a C_6H_6 solution of **3** into a 30 mL stainless steel bomb equipped with a stir bar to ensure rapid mixing of gas with the solution.[8] The bomb was placed in a 25 °C water bath and pressurized with 38 atm of CO. After 10 min, CO and solvent were rapidly evaporated and the residue was analyzed by ^{1}H NMR spectroscopy. Integration showed a 1.0:0.6 ratio of **3** to **8**. Assuming a first-order dependence on rhenium, the rate of appearance of **8** was determined ($k_{obs} = 8.3 \times 10^{-4}$ s^{-1}, $t_{1/2} = 14$ min). When the reaction of **3** with CO was carried out under 18 atm of CO, a similar rate was observed ($k_{obs} = 7.4 \times 10^{-4}$ s^{-1}, $t_{1/2} = 16$ min). Plots of k_{obs} versus CO pressure leveled off at high pressure (Figure 3). This analysis rests on the assumptions that the reaction is first order in **3** (as observed at low pressures) and *that the major species in solution is still* **3**. Several mechanisms might account for the rate leveling at higher CO pressure (>18 atm) will be discussed before a second and more accurate method of monitoring the rate of formation of **8** at CO pressures between 10 and 120 atm is presented.

The near linear increase in the rate of appearance of **8** versus CO pressure from 1 to 5 atm is consistent with an associative mechanism involving initial addition of CO to **3** followed by subsequent loss of alkyne to generate **8**. The near zero-order rate dependence on CO at higher pressure requires a change in the rate-determining step to one in which the major species present in solution reacts in a first-order process to generate an intermediate that is converted to product **8**. The first mechanism that we considered was an unprecedented non-nucleophile-assisted ring slippage to the η^3-indenyl intermediate **A** followed by trapping of the intermediate by CO to form **B** (Scheme 5). The η^3-indenyl intermediate **A** is suggested to be stabilized by the alkyne ligand which can switch from a 2e- to a 4e-donor as ring slippage occurs. At high CO pressure, intermediate **A** is efficiently trapped by CO to form **B** and the formation of **A** becomes the rate-determining step. A prediction of this mechanism is that at very high

(7) The concentration of CO in solution was calculated using the Ostwald coefficient: (a) *Solubility Data Series: Carbon Monoxide*; Cargill, R. W., Ed.; Pergamon Press: Oxford, U.K., 1990; Vol. 43, p 113. (b) Just, G. Z. *Phys. Chem., Stoechiom. Verwandtschaftsl.* **1901**, *37*, 342. (c) Park, J.; Yi, X.; Gasem, K. A. M.; Robinson, R. L., Jr. *J. Chem. Eng. Data* **1995**, *40*, 245.

(8) As a test for maintenance of the CO concentration in solution, the rates of reaction of **3** at 40 atm CO were run at 1.7 and 4.9 mM concentrations of **3**. If the reactions were CO starved, then the effect of CO starvation should have been more pronounced at the higher concentrations of **3** where CO depletion would be accentuated. However, similar rates were observed.

^{13}CO pressure no incorporation of ^{13}CO into recovered starting material will be observable. A second possible mechanism involves the buildup of an η^3- (**B**) or η^1-indenyl complex (**12**) at high CO pressure. Once the new species is the major species present, the pressure dependence on CO should disappear. This type of mechanism requires that the new species be detectable by direct monitoring of the reaction mixtures at high pressure.

The reaction of **3** with 10−120 atm of CO was monitored in a stainless steel pressure reactor equipped with a React-IR probe.[9] For example, when a solution of **3** in C_6H_6 in a stainless steel pressure reactor was placed under 68 atm of CO, IR carbonyl bands of **3** rapidly disappeared in 2−3 min and two new peaks not associated with **8** or **3** appear at 1946 and 1995 cm^{-1}. The new peaks slowly disappeared and peaks for **8** at 1927 and 2024 cm^{-1} appeared. A plot of $\ln(([\mathbf{8}]_{inf} - [\mathbf{8}])/[\mathbf{8}]_{inf})$ versus time was linear through 3 half-lives, indicating the appearance of **8** over time followed first-order kinetics ($k_{obs} = 9.5 \times 10^{-4}$ s^{-1}, $t_{1/2} = 12$ min). The rate of appearance of **8** was measured for a number of CO pressures between 10 and 120 atm of CO (Table 1, Figure 3). The rate of appearance of **8** showed an inverse dependence on CO pressure at these high pressures. The previous apparent leveling of the rate of formation of **8** at high CO pressure when the reactions were monitored by release of pressure and NMR analysis is now attributed to the inadequacy of this analysis procedure.

(η^1-C_9H_7)Re(CO)$_4$(η^2-MeC≡CMe) (12). While the ReactIR allowed us to observe a new major species (**12**) in the reaction of (η^5-C_9H_7)(CO)$_2$Re(η^2-MeC≡CMe) (**3**) with 68 atm of CO, we could not positively identify this species from an IR spectrum of a mixture of **8**, **3**, and **12**. However, ^1H NMR spectroscopy provides a very powerful method for differentiating between η^5-, η^3-, and η^1-indenyl binding modes to rhenium.[10]

In considering optimum conditions for NMR observation of the new species, we noted that the species was observable by IR spectroscopy only above ∼20 atm CO. Our hypothesis that the new species was either an η^3- or η^1-indenyl complex formed by addition of one or two CO ligands predicted that ΔS for the formation of the addition product would be strongly negative and adduct formation would be more favorable at low temperature. A solution of **3** in $C_6D_5CD_3$ was placed under 10 atm CO in a thick walled NMR tube and maintained at −15 °C for 6 h. The ^1H NMR spectrum at −65 °C showed that the solution contained (η^1-C_9H_7)Re(CO)$_4$(η^2-MeC≡CMe) (**12**) along with **8** and **3**. The structure of **12** is supported by the observation of seven new and distinct indenyl proton resonances as expected for an η^1-indenyl complex. The resonance for coordinated butyne in **12** appeared at δ 1.78; resonances for bound butyne of **3** (δ 2.10) and for free butyne (δ 1.62) were also seen. In the ^{13}C NMR spectrum, there were nine distinct resonances for indenyl carbons with the C1 resonance shifted to much lower frequency (δ 19.4) as observed for other η^1-indenyl rhenium complexes. Resonances at δ 55.4 and 11.1 for 2-butyne bound to **12**, resonances at δ 67.6 and 10.9 for 2-butyne bound to **3**, and resonances at δ 72.6 and −0.8 for free 2-butyne were also seen. We also observed one ^{13}C resonance in the rhenium carbonyl chemical shift region for **12** at δ 190.4 along with ^{13}C resonances for **3** (δ 204.1) and **8** (δ 194.2). While this method was useful for observing and identifying **12** in situ, the highest ratio of **12**:**8**:**3** observed was 30:20:50.

Higher enrichment of **12** was needed for measurement of the rate of loss of CO and alkyne from **12**. We succeeding in synthesizing a 92:4:4 mixture of **12**:**8**:**3** by cooling a $C_6D_5CD_3$ solution of **3** in a stainless steel pressure vessel at −10 °C, adding 100 atm of CO, stirring for 1 h, cooling to −78 °C, and then releasing pressure. The resulting solution of highly enriched **12** was transferred to NMR tubes cooled to −78 °C.

Stereochemistry of (η^1-C_9H_7)Re(CO)$_4$(η^2-MeC≡CMe) (12). ^{13}C NMR and IR spectroscopy established the trans relationship of the alkyne and η^1-indenyl ligands of **12**. In the ^{13}C NMR spectrum, only one ^{13}CO resonance at δ 190.4 was observed, consistent with the trans ligand assignment; the cis isomer has four different CO ligands. The IR spectrum had two CO bands at 1946 (br, m) and 1995 (s) cm^{-1}. Since the near C_{4v} symmetry of the trans isomer is broken by the alkyne ligand to approximate C_{2v} symmetry, two IR bands are expected. We suggest that the alkyne is aligned parallel to one pair of trans CO's and that the alkyne and this pair of CO's compete for back-bonding from the same metal d-orbital. The IR band for this pair of parallel CO's therefore appears at substantially higher frequency (1995 cm^{-1}) than the IR band (1946 cm^{-1}) for the pair of CO's perpendicular to the alkyne ligand. The alternative cis isomer would have near C_s symmetry, and three strong CO bands and a weak CO band would have been expected.

CO Loss from (η^1-C_9H_7)Re(CO)$_4$(η^2-MeC≡CMe) (12). Upon warming a $C_6D_5CD_3$ solution of **12** to −9 °C, conversion to a 12:1 mixture of alkyne complex **3** (δ 5.36) and tricarbonyl complex **8** (δ 5.70) was observed by ^1H NMR spectroscopy during the first half-life. The ratio of **3**:**8** decreased at longer times due to an increase in the amount of CO in solution released from **12**.

The rate of disappearance of the δ 4.5 ^1H NMR resonance of (η^1-C_9H_7)Re(CO)$_4$(η^2-MeC≡CMe) (**12**) was measured between −24 and 2 °C. The headspace of the NMR tube was left under vacuum to facilitate the removal of released CO. The rate was first order in **12** at −9 °C through 3 half-lives ($k_{obs} = 1.3 \times 10^{-4}$ s^{-1}, $t_{1/2} = 87$ min). Between −4 and 2 °C, the rate of disappearance of **12** was determined during the first half-life to avoid inhibition by released CO. An Eyring plot yielded activation parameters of $\Delta H^{\ddagger} = 17.9 \pm 1.0$ kcal mol^{-1} and $\Delta S^{\ddagger} = -8.3 \pm 3$ eu for the loss of CO from **12**. These activation parameters were used to estimate the rate of CO loss of **12** at 25 °C as 7.7×10^{-3} s^{-1} ($t_{1/2} = 1.5$ min).

Formation of (η^1-C_9H_7)Re(CO)$_5$ (13). At 100 atm of CO pressure, **8** reacts slowly with CO to form (η^1-C_9H_7)Re(CO)$_5$ (**13**). The rate of disappearance of the 1929 cm^{-1} band of **8** followed pseudo-first-order kinetics for over 3 half-lives ($k_{obs} = 4.76 \times 10^{-5}$ s^{-1}, $t_{1/2} = 4$ h, $\Delta G^{\ddagger} = 23.4$ kcal mol^{-1}). **13** was stable at room temper-

(9) A 30 mL PARR stainless steel pressure vessel equipped with a SiComp probe of a ASI ReactIR infrared spectrometer. SiComp probe is an attenuated total reflectance (ATR) device with silicon as the ATR surface.

(10) Chemical shift and the proton resonance pattern are distinctive for the three different modes of coordination. O'Connor, J. M.; Casey, C. P. *Chem. Rev.* **1987**, *87*, 307.

Table 2. Pressure Dependence of the Rate of Reaction of CO with (η^5-C_9H_7)$(CO)_2$Re(η^2-*cis*-MeHC=CHMe) (2) at 25 °C

CO (atm)	[CO] (mM)	[Re] (mM)	$k_{obs} \times 10^5$ (s^{-1})	$t_{1/2}$ (h)
2.0[a]	14	11	0.15	128
2.7[a]	19	7	0.23	84
4.1[a]	28	13	0.64	30
27.2[b]	190	5	1.9	10
40.8[b]	285	5	4.0	5
87[c]	606	5	7.4	2.6

[a] Rate measured by IR spectroscopy after release of CO pressure. [b] Reaction run in high-pressure reaction vessel and mixture analyzed by ^{1}H NMR spectroscopy after release of pressure. [c] Rate measured by in situ IR spectroscopy.

ature for days and lost CO to re-form **8** upon heating at 90 °C. The rate of disappearance of **13** at 90 °C ($t_{1/2}$ 10 min) was determined by monitoring the disappearance of its proton resonance (H1) at δ 3.9.

(η^1-C_9H_7)Re$(CO)_5$ (**13**) is kinetically much more robust than η^1-indenyl alkyne complex **12**, which loses CO rapidly at room temperature (rate extrapolated to 25 °C $= 7.7 \times 10^{-3}$ s^{-1}, $t_{1/2} = 1.5$ min). Similarly, addition of CO to (η^5-C_9H_7)Re$(CO)_3$ (**8**) to produce **13** is much slower than addition of CO to alkyne complex (η^5-C_9H_7)-Re$(CO)_2$(MeC≡CMe) (**3**). Thus, an alkyne complex not only accelerates CO addition to η^5-indenyl complexes but also accelerates CO dissociation from η^1-indenyl complexes. In Os$(CO)_4$(η^2-CF_3C≡CCF_3), the alkyne increases the labilization of CO ligands cis to the alkyne by a factor of 10^6 compared to the labilization of CO from the parent Os$(CO)_5$ complex.[11] Similar cis labilization of CO by the alkyne ligand in complex **12** explains the rapid loss of CO from **12**.

Pressure Dependence of the CO Substitution of Alkene Complex 2. The rate of reaction of CO with alkene complex **2** showed a linear dependence on CO pressure over the entire range from 1 to 87 atm (Table 2), in contrast to observations for alkyne complex **3**. When the reaction of **2** under 87 atm CO was monitored in situ by IR spectroscopy, no η^1-indenyl complex was observed and the rate of disappearance of **2** was the same as the rate of appearance of **8** ($k_{obs} = 7.4 \times 10^{-5}$ s^{-1}, $t_{1/2} = 2.6$ h).

The linear dependence on CO pressure is consistent with an associative process involving initial addition of CO to **2** followed by loss of alkene. The overall rate of CO addition and alkene loss is much slower than that of CO addition and alkyne loss.

Reaction of ^{13}CO with (η^5-C_9H_7)$(CO)_2$Re(η^2-MeC≡CMe) (3). The reaction of ^{13}CO with **3** was studied over the pressure range 1−15 atm. Reactions were run to completion, and the tricarbonyl complex (η^5-C_9H_7)Re-$(CO)_3$ (**8**) was isolated and its isotopic composition analyzed by electron impact mass spectrometry. The cluster of peaks at *m/e* 384−389 due to the isotopomers of **8** (37% ^{185}Re, 63% ^{187}Re) was used to determine the ^{13}C labeling pattern. The ratio of **8-(^{13}CO)$_1$**:**8-(^{13}CO)$_2$**:**8-(^{13}CO)$_3$** was determined by fitting the observed ratio of peaks in the 384−389 range as the weighted sum of the patterns calculated for one, two, or three ^{13}CO labels (Table 3). The expected isotopic patterns of **8-(^{13}CO)$_1$**:**8-(^{13}CO)$_2$**:**8-(^{13}CO)$_3$** took into account that the labeled carbon monoxide from Cambridge Isotope Laboratories contained approximately 10% of $^{13}C^{18}O$ along with 90% $^{13}C^{16}O$. A significant increase in multiply labeled **8** was seen as the ^{13}CO pressure was raised.

Table 3. ^{13}CO Label in (η^5-C_9H_7)Re$(CO)_3$ (8) after Complete Reaction of 3 with ^{13}CO

pressure (atm)	% **8-(^{13}CO)$_1$**	% **8-(^{13}CO)$_2$**	% **8-(^{13}CO)$_3$**
1	67 ± 6	23 ± 4	10 ± 6
2	72 ± 6	20 ± 4	8 ± 6
3	54 ± 6	30 ± 4	16 ± 6
4	45 ± 6	31 ± 4	24 ± 6
5.3	45 ± 6	30 ± 4	25 ± 6
15	32 ± 6	26 ± 4	43 ± 6

Table 4. ^{13}CO Incorporation into (η^5-C_9H_7)$(CO)_2$Re(η^2-MeC≡CMe) (3) after ~50% Conversion to (η^5-C_9H_7)Re$(CO)_3$ (8)

^{13}CO pressure (atm)	**8**	% **3-(^{13}CO)$_0$**	% **3-(^{13}CO)$_1$**	% **3-(^{13}CO)$_2$**	% ^{13}CO in **3**:% **8**
1	46%	77 ± 4	18 ± 4	4 ± 4	0.26
2	49%	65 ± 4	24 ± 4	12 ± 4	0.37
3	50%	62 ± 4	24 ± 4	13 ± 4	0.37
4	46%	64 ± 4	23 ± 4	14 ± 4	0.43
12	29%	64 ± 4	22 ± 4	14 ± 4	0.88

Table 5. ^{13}CO Label in (η^5-C_9H_7)Re$(CO)_3$ (8) after 50% Conversion of 3

^{13}CO pressure (atm)	conversion to **8**	% **8-(^{13}CO)$_1$**	% **8-(^{13}CO)$_2$**	% **8-(^{13}CO)$_3$**
1	46%	91 ± 6	8 ± 4	1 ± 6
2	49%	82 ± 6	12 ± 4	6 ± 8
3	50%	83 ± 6	12 ± 4	7 ± 6
3.6	42%	89 ± 6	8 ± 4	3 ± 6
4	46%	82 ± 6	12 ± 4	6 ± 6
12	29%	82 ± 6	12 ± 4	6 ± 6
13	50%	65 ± 6	23 ± 4	12 ± 6

The appearance of multiple labels in tricarbonyl product **8** could have resulted from exchange into starting material **3** during the course of reaction, from exchange into a reactive intermediate during the conversion of **3** to **8**, or from exchange into product **8**. A control experiment excluded exchange into product **8** under the reaction conditions. Treatment of a C_6D_6 solution of **8** with 5 atm of ^{13}CO for 2 days at room temperature showed no change in the ^{13}C NMR spectrum. This requires that exchange of ^{13}CO into **8** be at least 500 times slower than the conversion of **3** to **8**.

The reaction of **3** with ^{13}CO was followed by ^{13}C NMR spectroscopy to determine if the label was incorporated into **3** during the course of reaction. When the reaction of **3** with 4.2 atm of ^{13}CO at 25 °C was followed by ^{13}C NMR spectroscopy, the ^{13}CO resonance of **3** at δ 204.1 initially increased at a rate similar to that of the ^{13}CO resonance for **8** at δ 194.3. This indicated roughly comparable rates of ^{13}CO exchange into **3** and of conversion of **3** to **8**. In another set of experiments using various ^{13}CO pressures, the reactions of **3** with ^{13}CO were stopped after about 50% conversion, and both **8** and **3** were isolated by thin-layer chromatography and analyzed by mass spectrometry (Tables 4 and 5).

Significant ^{13}CO incorporation into recovered **3** (23−50%, depending on pressure) was seen after about 50% conversion to **8** and ^{13}CO incorporation into **3** increased somewhat as the ^{13}CO pressure was raised. The relative rate of ^{13}CO incorporation into **3** compared with conversion of **3** to **8** is given by {[**3-(^{13}CO)$_1$**] + [**3-(^{13}CO)$_2$**]}/[**8**] and increased with CO pressure (Table 4). Figure 4 is

(11) Pearson, J.; Cooke, J.; Takats, J.; Jordan, R. B. *J. Am. Chem. Soc.* **1998**, *120*, 1434.

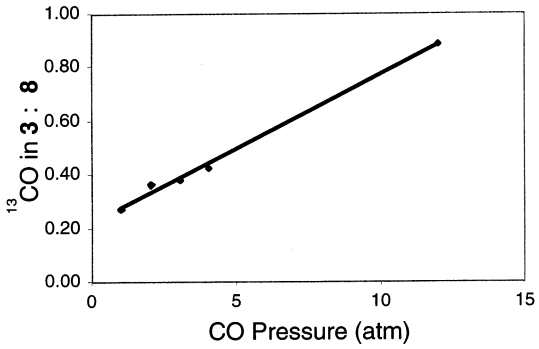

Figure 4. CO pressure dependence of the relative rates of ^{13}CO incorporation into **3** compared with conversion of **3** to **8**. The relative rate is given by the ratio of {[**3**-(^{13}CO)$_1$]- + [**3**-(^{13}CO)$_2$]}:[**8**] at partial conversion of **3** to **8**.

Scheme 6

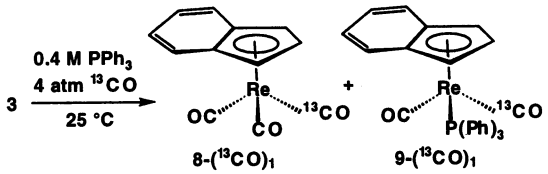

consistent with a combination of pressure-independent and pressure-dependent routes for this rate ratio.

PPh_3 Trapping of Reactive Intermediates in the CO Substitution of (η^5-C_9H_7)$(CO)_2$Re(η^2-MeC≡CMe) (3). In an effort to trap intermediates in the reaction of (η^5-C_9H_7)$(CO)_2$Re(η^2-MeC≡CMe) (**3**) with CO, we studied carbonylation in the presence of PPh_3. We first explored the reaction of PPh_3 with **3** without added CO. The reaction of **3** with PPh_3 in C_6D_6 at 25 °C slowly produced the known phosphine complex (η^5-C_9H_7)$(CO)_2$-Re(PPh_3).[12] The rate of disappearance of **3** was monitored by ^{1}H NMR spectroscopy following the disappearance of the resonance at δ 2.05 of the 2-butyne ligand. The rate was first order in rhenium and first order in PPh_3 ($k_{obs} = 8.6 \times 10^{-7}$ s^{-1}, $t_{1/2} = 225$ h, 0.21 M PPh_3; $k_{obs} = 17 \times 10^{-7}$ s^{-1}, $t_{1/2} = 113$ h, 0.41 M PPh_3). Basolo previously showed that (η^5-C_9H_7)Re$(CO)_3$ reacts with phosphines through an associative mechanism to give (η^5-C_9H_7)$(CO)_2$Re(phosphine) and suggested an indenyl ring slip mechanism for the reaction.[13] Significantly, the reaction of **3** with PPh_3 was more than 100 times slower than the reaction of **3** with CO.

Under 4 atm ^{13}CO, the reaction of **3** with 0.42 M PPh_3 at 25 °C was greatly accelerated and a 1.0:5.0 mixture of (η^5-C_9H_7)Re$(CO)_3$ (**8**):(η^5-C_9H_7)Re$(CO)_2$Re(PPh_3) (**9**) was formed (Scheme 6). Surprisingly, the disappearance of **3** was faster for the system with both ^{13}CO and PPh_3 ($k_{obs} = 5.1 \times 10^{-4}$ s^{-1}, $t_{1/2} = 22$ min, 0.42 M PPh_3, 4 atm CO) than the reaction with only PPh_3 ($k_{obs} = 1.7 \times 10^{-6}$ s^{-1}, $t_{1/2} = 113$ h, 0.41 M PPh_3) or only ^{13}CO present ($k_{obs} = 1.5 \times 10^{-4}$ s^{-1}, $t_{1/2} = 66$ min, 4.1 atm CO).

Both **8** and **9** were isolated by TLC and analyzed by mass spectrometry to determine the amount of ^{13}CO incorporation into each. (η^5-C_9H_7)Re$(CO)_3$ (**8**) showed significant multiple labeling: 43 ± 6% **8**-(^{13}CO)$_1$:38 ± 6% **8**-(^{13}CO)$_2$:19 ± 6% **8**-(^{13}CO)$_3$. Multiple labeling was also seen for phosphine complex **9**: 35 ± 4% **9**-(^{13}CO)$_0$: 44 ± 4% **9**-(^{13}CO)$_1$:21 ± 4% **9**-(^{13}CO)$_2$.

Scheme 7

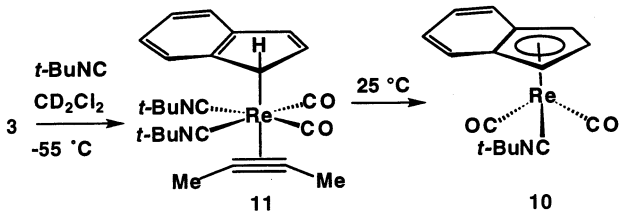

The cooperativity between CO and PPh_3 in accelerating the rate of disappearance of **3** is consistent with PPh_3 trapping of a reactive intermediate reversibly formed during the reaction of **3** with CO. The high concentration of phosphine in solution leads to more efficient trapping of this reactive intermediate than when ^{13}CO is the only trapping agent present. The sequential addition of ^{13}CO and PPh_3 generates an intermediate that then loses alkyne and either CO or ^{13}CO. This explains the high incorporation of ^{13}CO into **9**.

Formation of (η^1-C_9H_7)Re$(CO)_2$(CN*t*-Bu)$_2$(η^2-MeC≡CMe) (11). *t*-BuNC is isoelectronic with CO and often is used as a model for CO; unlike CO, it is easy to obtain high concentrations of *t*-BuNC in solution. The reaction of **3** with *t*-BuNC was investigated for comparison with the reaction of **3** with CO. Treatment of a CD_2Cl_2 solution of alkyne complex **3** with slightly less than 1 equiv of *t*-BuNC (0.2 M) at room temperature for several hours led to the formation of the *t*-BuNC substitution product (η^5-C_9H_7)$(CO)_2$Re(CN*t*-Bu) (**10**) (Scheme 7). The ^{1}H NMR spectrum of **10** showed typical η^5-indenyl shifts at δ 7.43 (m), 7.02 (m), 5.64 (d), and 5.53 (t) for the ring hydrogens as well as a singlet at δ 1.35 for the *t*-BuNC ligand.

When the reaction of **3** with less than 1 equiv of *t*-BuNC was carried out in CD_2Cl_2 at −78 °C, rapid formation of the η^1-indenyl complex (η^1-C_9H_7)Re$(CO)_2$-(CN*t*-Bu)$_2$(η^2-MeC≡CMe) (**11**) was observed. The ^{1}H NMR spectrum at −70 °C showed only starting alkyne complex **3** and η^1-indenyl complex **11** in solution. The ^{1}H NMR spectrum of **11** showed two resonances at δ 1.45 and 1.42 for the diastereotopic *t*-BuNC ligands, an alkyne methyl resonance at δ 2.41, and seven distinct indenyl resonances for the η^1-indenyl hydrogens. Subsequent warming of the solution to room temperature for several hours resulted in the formation of *t*-BuNC complex **10**.[14]

The ^{1}H NMR spectrum of η^1-indenyl complex **11** at room temperature showed evidence for a fluxional process involving a 1,3 shift of the η^1-indenyl ligand. This process interchanges the environments of the indenyl hydrogens and results in the coalescence of the seven resonances seen at low temperature to four broad resonances at δ 7.41, 6.94, 6.33, and 4.35. The fluxional process also interchanges the environments of the *t*-BuNC ligands seen at δ 1.43. The stereochemistry shown for **11** is consistent with the observation of two *t*-BuNC resonances and a single 2-butyne methyl resonance at low temperature and with the observation of a single *t*-BuNC resonance at room temperature.

(12) Kolobova, N. E.; Lobanova, I. A.; Zdanovich, V. I.; Petrovskii, P. V. *Izv. Akad. Nauk SSSR, Ser. Khim.* **1981**, *5*, 935.

(13) Bang, H.; Lynch, T. J.; Basolo, F. *Organometallics* **1992**, *11*, 40.

(14) Addition of excess CN*t*-Bu to **3** in an effort to obtain complete conversion led to formation of uncharacterized decomposition products.

Scheme 8

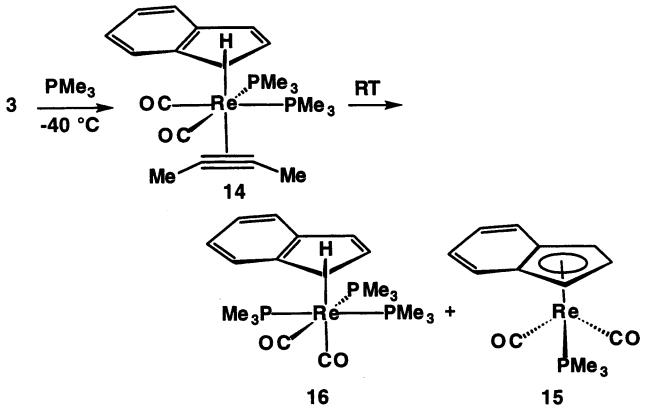

Formation of (η^1-C_9H_7)Re(CO)$_2$(PMe$_3$)$_2$(η^2-MeC≡CMe) (14). Addition of PMe$_3$ to alkyne complex **3** occurred at −40 °C to give (η^1-C_9H_7)Re(CO)$_2$(PMe$_3$)$_2$(η^2-MeC≡CMe) (**14**), which was isolated by low-temperature evaporation of solvent (Scheme 8). **14** was unstable at room temperature but was shown to be formed in 90% yield by low-temperature NMR of the redissolved solid. The $^{13}C\{^1H\}$ NMR spectrum had two CO resonances, each with one large coupling to a trans phosphine and one small coupling to a cis phosphine that established the stereochemistry of **14**. Upon warming to room temperature, **14** lost 2-butyne and formed a 1:2 mixture of (η^5-C_9H_7)Re(CO)$_2$(PMe$_3$) (**15**) and (η^1-C_9H_7)Re(CO)$_2$-(PMe$_3$)$_3$ (**16**).[15]

Pure **16** was obtained from reaction of **3** with excess PMe$_3$ at room temperature. The η^1-indenyl ligand of **16** shows separate resonances for H1 and H3 at low temperature, but a fluxional process causes coalescence of these peaks at 0 °C ($\Delta G^{\ddagger} = 11.8$ kcal mol^{-1}). In the low-temperature ^{31}P NMR spectrum of **16**, resonances are seen for nonequivalent diastereotopic trans phosphines at δ −17.0 (dd, $J = 156$, 26 Hz) and −20.5 (dd, $J = 156$, 26 Hz) and for a third phosphine at δ −28.2 (t, $J = 26$ Hz). The ^{13}C NMR resonance at δ 200.9 (dt, $J_{P-C} = 60$, 8 Hz, CO) establishes that one CO is trans to a phosphine ligand, while the resonance at δ 195.7 (q, $J_{P-C} = 8$ Hz CO) is assigned to CO trans to the η^1-indenyl ligand and cis to three phosphines.

Discussion

We will focus on three significant aspects of this work: (1) the unique cooperativity between alkyne and indenyl ligands in promoting substitution reactions, (2) insight into the details of alkyne substitution gained from kinetic and ^{13}CO labeling studies, and (3) CO-catalyzed phosphine substitution.

Indenyl Effect on CO Substitution of Alkyne and Alkene Complexes. The rate of the CO substitution reactions of indenyl alkene and alkyne complexes displayed a linear dependence on CO pressure up to 10 atm that provided evidence for an associative mechanism. The rates of the indenyl substitutions were much faster than those of their Cp analogues. While the Cp alkene complex **4** did not react under 4 atm CO up to 80 °C, the indenyl alkene complex **2** reacted under 4 atm CO at 25 °C ($t_{1/2} = 30$ h). This corresponds to a difference in activation barriers of more than 7.5 kcal mol^{-1}. While the Cp alkyne complex **5** barely reacted under 4 atm CO at 25 °C (only 3% reaction after 24 days), the indenyl alkyne complex **3** reacted quickly under 4 atm CO at 25 °C ($t_{1/2} = 66$ min). This corresponds to a difference in activation barriers of more than 5 kcal mol^{-1}. These large rate increases are a signature of an indenyl effect occurring in the CO substitution reactions of **2** and **3** and support formation of a ring-slipped intermediate in these associative substitutions.

Indenyl and Alkyne Ligand Cooperativity. The combination of the indenyl ligand along with the alkyne ligand of **3** led to uniquely fast rates of CO substitution. Both indenyl and alkyne ligands are variable electron donors: the indenyl ligand can slip from an η^5 6e-donor to an η^3 4e-donor,[4,16] while the alkyne ligand can switch from a 2e- to a 4e-donor ligand.[17] Ring slippage of Cp and indenyl ligands allows associative addition of a new ligand while maintaining an 18e count at the metal. Indenyl ligands slip more readily than Cp ligands because of their inherently weaker binding as η^5 ligands and because of their greater stability as η^3 ligands due to the increased aromaticity of the six-membered ring in the slipped indenyl intermediate.[3−5]

Acceleration of ligand dissociation by alkyne ligands has been attributed to the alkyne ligand's ability to switch to a 4e-donor mode and stabilize a developing "vacant" coordination site. Wulff suggested that coupling of a carbene ligand with CO to give a vinyl ketene might be promoted by a coordinated alkyne changing from a 2e- to a 4e-donor.[18] Takats suggested that the alkyne osmium complex Os(CO)$_4$(η^2-MeC≡CMe) loses CO prior to reacting with a second alkyne and the intermediate formed from loss of CO is stabilized by the alkyne ligand changing from a 2e- to a 4e-donor.[19] Takats and Jordan found that Os(CO)$_4$(η^2-CF_3C≡CCF_3) reacts with phosphines by a dissociative mechanism at a rate 10^6 times faster than Os(CO)$_5$.[11]

The CO substitution of indenyl alkyne complex **3** takes advantage of both the indenyl and alkyne ligand rate-enhancing effects to give even faster rates than those attributed to having just one of the ligands. This ligand cooperativity might be due to simultaneous indenyl ring slippage and a switch of the alkyne ligand from a 2e- to a 4e-donor; in this extreme, an intermediate **A** would be reversibly formed and trapped by CO at a rate that never approaches the saturation limit (Scheme 5). An alternative explanation of the cooperativity involves concerted CO attack and ring slippage, with the electron-deficient transition state being stabilized by the additional electron donation from the alkyne ligand. These alternatives are not kinetically distinguishable.

Kinetic Evidence for the Broad Outlines of the Mechanism of CO Substitution of Alkyne Complex 3. The rate of conversion of alkyne complex **3** to CO

(15) The ratio of (η^5-C_9H_7)Re(CO)$_2$(PMe$_3$) (**15**) and (η^1-C_9H_7)Re(CO)$_2$-(PMe$_3$)$_3$ (**16**) was not 1:1 as expected from stoichiometry because there was still approximately 0.8 equiv of free PMe$_3$ left in solution after removing the solvent from (η^1-C_9H_7)Re(CO)$_2$(PMe$_3$)$_2$(η^2-MeC≡CMe) (**14**) and redissolving in CD_2Cl_2.

(16) Ji, L.-N.; Rerek, M. E.; Basolo, F. *Organometallics* **1984**, *3*, 740.
(17) Templeton, J. L. *Adv. Organomet. Chem.* **1989**, *29*, 1.
(18) Bos, M. E.; Wulff, W. D.; Miller, R. A.; Chamberlin, S.; Brandvold, T. A. *J. Am. Chem. Soc.* **1991**, *113*, 9293.
(19) Washington, J.; McDonald, R.; Takats, J.; Menashe, N.; Reshef, D.; Shvo, Y. *Organometallics* **1995**, *14*, 3996.

substitution product **8** depends linearly on CO pressure. At low CO pressure (1−10 atm), rate = k_{1obs}[**3**][CO]; k_{1obs} = 4.45×10^{-5} atm^{-1} s^{-1} at 25 °C. At higher CO pressure the rate of disappearance of starting material **3** continued to increase, but the formation of significant quantities of η^1-indenyl complex **12** complicated analysis of the kinetics at higher CO pressure.

The η^1-indenyl complex **12** was prepared in 90% yield under high CO pressure at low temperature. In the absence of added CO pressure, **12** reacted to generate a 12:1 ratio of starting alkyne complex **3**:CO substitution product **8**. This partitioning requires that $k_{1obs} = k_1[k_3/(k_3 + k_{-1})] = k_1[1/13]$ and gives the rate constant $k_1 = 5.8 \times 10^{-4}$ atm^{-1} s^{-1} at 25 °C for the conversion of **3** to η^3-indenyl intermediate **B** (Scheme 9).

As detailed earlier, we independently measured the rate of CO loss from **12** in the absence of added CO between −24 and 2 °C. Extrapolation of the Eyring plot to 25 °C gave an estimate of the first-order rate constant for loss of CO from **12** of $k_{-2} = 7.7 \times 10^{-3}$ s^{-1} at 25 °C. The rate of CO loss from η^1-indenyl alkyne complex **12** was approximately 10^6 times faster than from the all-carbonyl η^1-indenyl complex (**13**). This remarkable rate acceleration is attributed to the ability of the alkyne ligand to facilitate CO loss by switching from 2e- to 4e-donor in the transition state for CO loss.[11,17,19]

In principle, η^1-indenyl complex **12** could lose alkyne first to form intermediate **C**, which could then lose CO to form **8**. Apparently this is not a significant pathway since ∼92% of **12** loses 2 CO's to re-form alkyne complex **3**. Detailed kinetic analysis also demonstrates that alkyne loss occurs from η^3-indenyl complex **B** and not from η^1-indenyl complex **12**. The rate law shown in eq 1 describes the reactions in Scheme 9. If 2-butyne were lost only from **12** ($k_4 \gg k_3 \approx 0$), eq 1 simplifies to eq 2 and the rate of appearance of **8** would depend on the square of the CO pressure at low CO pressure. However, a linear CO dependence was observed at pressures below 10 atm of CO. Therefore, loss of alkyne from **12** is not an important process at low CO pressure.

$$\frac{d[\mathbf{8}]}{dt} = \frac{k_1 k_3[CO][\mathbf{3}]}{k_{-1} + k_3 + k_2[CO]} + \frac{k_{-2} k_3[\mathbf{12}]}{k_{-1} + k_3 + k_2[CO]} + k_4[\mathbf{12}] \quad (1)$$

if $k_3 = 0$ and [**3**] ≫ [**12**]

$$\frac{d[\mathbf{8}]}{dt} = \frac{k_1 k_2 k_4[CO]^2[\mathbf{3}]}{(k_{-1} + k_2[CO])(k_{-2} + k_4)} \quad (2)$$

if $k_4 = 0$ and [**3**] ≫ [**12**]

$$\frac{d[\mathbf{8}]}{dt} = \frac{k_1 k_3[CO][\mathbf{3}]}{k_{-1} + k_3} \quad (3)$$

if $k_3 = 0$ and [**12**] ≫ [**3**]

$$\frac{d[\mathbf{8}]}{dt} = k_4[\mathbf{12}] \quad (4)$$

if $k_4 = 0$ and [**12**] ≫ [**3**]

$$\frac{d[\mathbf{8}]}{dt} = \frac{k_{-2} k_3[\mathbf{12}]}{k_3 + k_2[CO]} \quad (5)$$

if $k_4 = 0$ and [**12**] ≫ [**3**]

$$\frac{1}{k_{obs}} = \frac{k_2[CO]}{k_{-2} k_3} + \frac{1}{k_{-2}} \quad (6)$$

We will consider two pathways for 2-butyne loss under high CO pressure where η^1-indenyl complex **12** is the major species. If complex **12** is the major species that loses butyne ($k_4[\mathbf{12}] \gg k_3[\mathbf{B}]$), the rate of appearance of **8** should be independent of CO pressure (eq 4). If intermediate **B** is the only complex that loses butyne, the rate expression for the appearance of **8** simplifies to eq 5, which has an inverse dependence on CO pressure. Experimentally, the rate of appearance of **8** was inversely dependent on CO pressure at pressures > 50 atm of CO where the major species in solution was **12**. Therefore, we conclude that butyne loss occurs from **B** and not from **12**, consistent with the low-pressure limit of losing butyne from **B**.

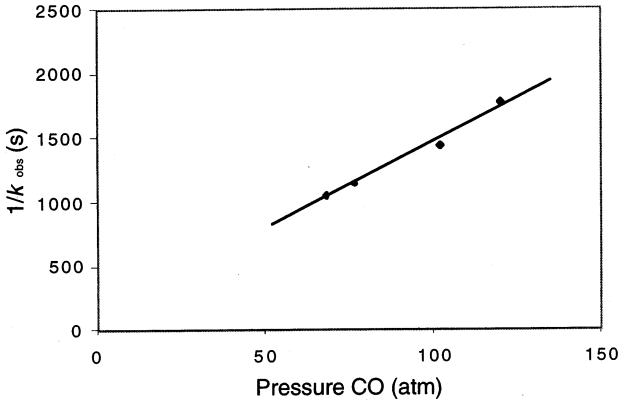

Figure 5. Plot of $1/k_{obs}$ for conversion of **12** to (η^5-C_9H_7)-$Re(CO)_3$ (**8**) vs pressure of CO above 68 atm.

The intercept of the plot of $1/k_{obs}$ versus CO pressure for conversion of **12** to **8** at pressures above 50 atm gives $k_{-2} = 8.8 \times 10^{-3}$ s^{-1} at 25 °C, which is the rate constant for CO dissociation from **12** (Figure 5 and eq 6). As detailed earlier, we independently measured the rate of CO loss from **12** in the absence of added CO between −24 and 2 °C. Extrapolation of the Eyring plot to 25 °C gave an estimate of k_{-2} as 7.7×10^{-3} s^{-1}, in close agreement with the measurement from Figure 5. The slope of the plot in Figure 5 gives $k_2/k_{-2}k_3 = 13.6$ atm^{-1} s^{-1}. This allows calculation of $k_2/k_3 = 0.12$ atm^{-1} with $k_{-2} = 8.8 \times 10^{-3}$ s^{-1}.

The observation that (η^1-indenyl)Re$(CO)_5$ (**13**) was not detected by IR during the conversion of **12** to **8** under high CO pressure is also consistent with the failure of **12** to lose butyne. If **12** lost butyne to generate intermediate **C**, trapping of **C** by CO would have given **13**, which is kinetically stable at 25 °C.

Refinement of the CO Substitution Mechanism Using ^{13}CO Labeling Data. The observation of extensive ^{13}CO incorporation into **3** at ∼50% conversion of **3** to **8** requires reversibility of the CO addition to **3** to give an η^3-indenyl intermediate **B** (Table 4). Loss of CO from **B** was independently established by the observation that the major reaction of **B** (generated by CO loss from η^1-indenyl complex **12**) was loss of a second CO to generate **3**.

The quantitative extent of ^{13}CO incorporation into **3** provides insight into the stereochemistry of **B**. Since we know that **B** loses CO to form **3** about 12 times more rapidly than it loses alkyne to form **8**, if ^{13}CO entered **B** randomly or if label scrambled in **B**, then at 50% conversion to **8**, the rhenium complexes would have had to cycle through **B-(^{13}CO)$_1$** six times and two-thirds of it would have lost CO and led to **3-(^{13}CO)$_1$**. This would have resulted in incorporation of multiple ^{13}CO ligands into **3**, but **3** recovered from reaction with 1 atm ^{13}CO

Scheme 9

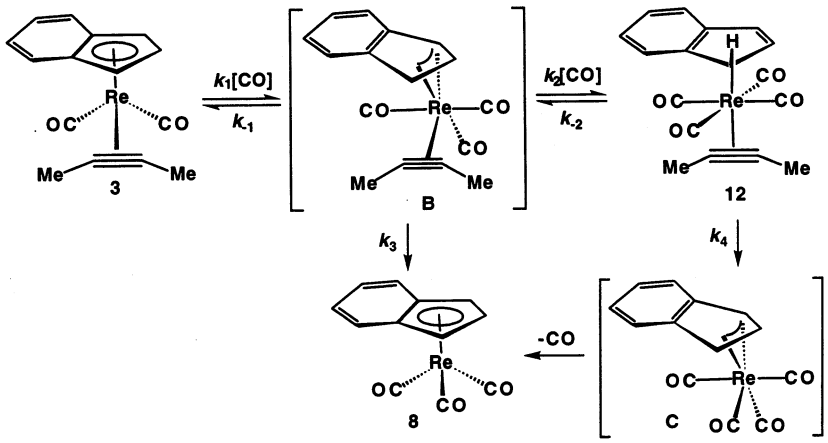

Scheme 10

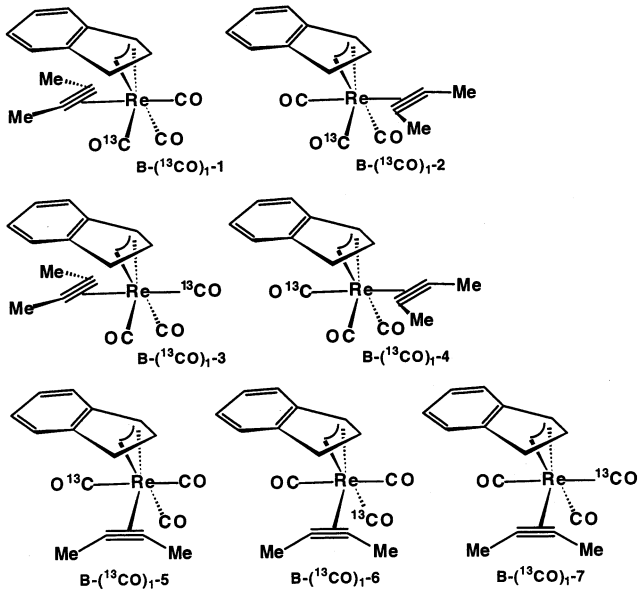

contained only 18% **3-(^{13}CO)$_1$** and 4% **3-(^{13}CO)$_2$**. Clearly, ^{13}CO does not enter **B** randomly. There are three different isomers of unlabeled **B** with different relationships between the alkyne and η^3-indenyl ligand and seven total isomers of **B-(^{13}CO)$_1$** shown in Scheme 10. If one of the two isomers with symmetry-related CO and ^{13}CO ligands (**B-(^{13}CO)$_1$-1** or **B-(^{13}CO)$_1$-2**) were the only isomer formed, microscopic reversibility would lead to ^{13}CO exchange into **3** one out of two times that **B** is generated; this would have resulted in incorporation of multiple ^{13}CO ligands into **3**, which was not seen. Therefore, **B-(^{13}CO)$_1$-1** and **B-(^{13}CO)$_1$-2** can be excluded as the major isomer of **B**. If one of the other five isomers (**B-(^{13}CO)$_1$-3**, **-4**, **-5**, **-6**, or **-7**) were the only isomer formed, microscopic reversibility would lead to no exchange.

Our data can be accommodated in two different ways. One possibility is that one of these five isomers is the major species generated by ^{13}CO addition to **3** and that it has a second minor mode of dissociating CO (and by microscopic reversibility, a second minor mode of adding CO). In this scenario, the two isomers have the same relationship between the alkyne and η^3-indenyl ligands (for example, major species **B-(^{13}CO)$_1$-3** and minor species **B-(^{13}CO)$_1$-1**). A second possibility involves one of the five isomers as the major species which does not give rise to ^{13}CO exchange and one of the two isomers with symmetrically related ^{13}CO and CO ligands as the minor species which is solely responsible for exchange. In this case, ^{13}CO enters and leaves only one site to generate each of the two isomers, and the two isomers are not required to have the same relationship between the alkyne and η^3-indenyl ligands (for example, major species **B-(^{13}CO)$_1$-3** and minor species **B-(^{13}CO)$_1$-2**).

Additional information about the likely stereochemistry of **B** comes from the conversion of **B** to the η^1-indenyl complex **12**, in which the indenyl and alkyne ligands are trans. The only isomers of **B** that can lead to **12** by CO replacement of the η^3-indenyl with retention of stereochemistry are the three isomers **B-(^{13}CO)$_1$-5**, **-6**, and **-7**. The two incoming ^{13}CO ligands in **12-(^{13}CO)$_2$** are likely to be cis to one another, since this is the stereochemistry seen in the η^1-indenyl PMe_3 complex **14** and the η^1-indenyl isonitrile complex **11**. It is interesting to note that the stereochemistry of these η^1-indenyl complexes results from CO substitution with retention of stereochemistry as the indenyl ring slips.

So far, we have discussed only routes to labeled **3** via η^3-indenyl intermediate **B**, but routes involving η^1-indenyl complex **12** also need to be considered. We will first consider whether routes through **12** are the only pathway to labeled **3**. If **12** with trans ^{13}CO ligands were formed selectively, microscopic reversibility would require loss of either two trans CO or two trans ^{13}CO ligands to give only **3-(^{13}CO)$_2$** and **3**. This possibility is clearly excluded since much more monolabeled **3-(^{13}CO)$_1$** was observed than doubly labeled **3-(^{13}CO)$_2$**. If **12** were formed with cis ^{13}CO ligands, microscopic reversibilty would require loss of cis CO ligands and would have given a 2:1 ratio of **3-(^{13}CO)$_1$**: **3-(^{13}CO)$_2$**. Under 1 atm ^{13}CO, the observed 4.5:1 ratio of **3-(^{13}CO)$_1$**: **3-(^{13}CO)$_2$** at 50% conversion to **8** is too low for ^{13}CO exchange into **3** to involve only routes through **12**.

We next considered whether the amount of **3-(^{13}CO)$_2$** can be explained solely via sequential exchange passing through monolabeled **3-(^{13}CO)$_1$**. Under 1 atm ^{13}CO, at 46% conversion of **3** to **8**, 9.7% **3-(^{13}CO)$_1$** had formed; sequential labeling predicts that only 0.5% **3-(^{13}CO)$_2$** should have been seen instead of the 2.1% observed. At higher ^{13}CO pressures, there are larger discrepancies: under 12 atm, at 29% conversion of **3** to **8**, 15.6% **3-(^{13}CO)$_1$** and 9.9% **3-(^{13}CO)$_2$** had formed, but sequential labeling predicts formation of only 0.8% **3-(^{13}CO)$_2$**.

Scheme 11

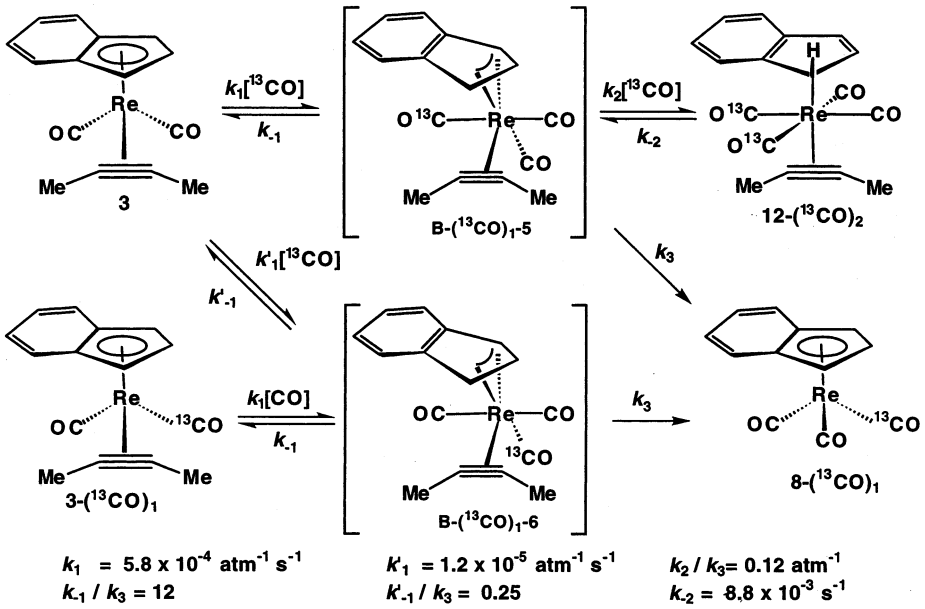

Clearly, (1) sequential reactions cannot alone account for the amount of double label seen and (2) a second direct route to double labeling becomes more important as ^{13}CO pressure is increased. This suggests that there are two routes to ^{13}CO exchange, one involving at least two different isomeric η^3-indenyl intermediates **B** and another involving cis **12-(^{13}CO)$_2$**, which becomes increasingly important at higher pressure.

A plot of the ratio of the sum of **3-(^{13}CO)$_1$** + **3-(^{13}CO)$_2$**:**8** versus CO pressure provides semiquantitative evidence for two pathways for ^{13}CO incorporation into **3** (Figure 4). The nonzero intercept is due to pressure-independent ^{13}CO incorporation into **3** via isomers of **B**, while the positive slope indicates a pressure-dependent pathway via η^1-indenyl intermediate **12**. The intercept indicates the rate of CO loss from intermediate **B** is about 0.25 as fast as alkyne loss. Assuming cis ^{13}CO in **12**, ^{13}CO incorporation into **3** will occur 75% of the time that **12** is formed and the slope of Figure 4 is $0.75 \times k_2/k_3 = 0.055$ atm^{-1}. This allows calculation of $k_2/k_3 = 0.075$ atm^{-1}. This ratio is similar to the value of 0.12 atm^{-1} calculated from the graph of $1/k_{obs}$ versus CO pressure for the observed rate of formation of **8** from **12** at CO pressures above 50 atm (Figure 5).

A mechanism that explains all of the facets described above and that gives a reasonable quantitative agreement with our data is shown in Scheme 11 with the indicated relative rate constants. (There are, of course, other combinations of isomers of **B-(^{13}CO)$_1$** that would also explain the data.) In this mechanism, ^{13}CO addition to **3** produces mainly intermediate **B-(^{13}CO)$_1$-5** by partial displacement of the indenyl ligand with retention of stereochemistry and a smaller amount of **B-(^{13}CO)$_1$-6**, which can lose CO to form **3-(^{13}CO)$_1$**. Addition of a second ^{13}CO to **B-(^{13}CO)$_1$-5** leads to cis **12-(^{13}CO)$_2$** and can account for excess double label **3-(^{13}CO)$_2$** at early reaction time and at higher pressure.

This reaction scheme and relative rate constants were used to simulate the time course of the formation of labeled **3** and **8** under 1, 4, and 12 atm ^{13}CO. Reasonable agreement was obtained for the labeling pattern in compound **3**, but the simulation systematically overestimated the amount of double labeled **8-(^{13}CO)$_2$**. For 1 atm, the labeling patterns (observed, *simulated*) were **3-(^{13}CO)$_0$** (77%, *75%*), **3-(^{13}CO)$_1$** (18%, *20%*), **3-(^{13}CO)$_2$** (4%, *5%*); and **8-(^{13}CO)$_1$** (91%, *80%*), **8-(^{13}CO)$_2$** (8%, *19%*), **8-(^{13}CO)$_3$** (1%, *2%*). For 4 atm, the labeling patterns (observed, *simulated*) were **3-(^{13}CO)$_0$** (64%, *69%*), **3-(^{13}CO)$_1$** (22%, *19%*), **3-(^{13}CO)$_2$** (14%, *13%*); and **8-(^{13}CO)$_1$** (82%, *72%*), **8-(^{13}CO)$_2$** (12%, *20%*), **8-(^{13}CO)$_3$** (6%, *6%*). For 12 atm, the labeling patterns (observed, *simulated*) were **3-(^{13}CO)$_0$** (64%, *69%*), **3-(^{13}CO)$_1$** (22%, *19%*), **3-(^{13}CO)$_2$** (14%, *13%*); and **8-(^{13}CO)$_1$** (82%, *79%*), **8-(^{13}CO)$_2$** (12%, *17%*), **8-(^{13}CO)$_3$** (6%, *1%*).

CO-Catalyzed Phosphine Substitution. The phosphine substitution of the indenyl alkyne complex **3** to form phosphine complex **9** was much faster in the presence of ^{13}CO, indicating that CO catalyzed the phosphine substitution of **3**.[20] The rate of reaction of **3** with PPh_3 in the absence of added CO depended on [PPh_3], which is consistent with an associative mechanism involving indenyl ring slippage. When ^{13}CO was added to the system, the rate of formation of phosphine complex **9** occurred several hundred times faster. The disappearance of **3** was about 3 times faster ($t_{1/2} = 22$ min vs $t_{1/2} = 66$ min) in the presence of ^{13}CO and PPh_3 than in the presence of ^{13}CO alone.

These results are explained in terms of the mechanism shown in Scheme 12. In the absence of added CO, PPh_3 slowly attacks **3** to form the phosphine-substituted η^3-indenyl intermediate **E**, which can lose alkyne to form the phosphine substitution product **9**. Interestingly, neither an η^5-indenyl phosphine alkyne complex nor an η^5-indenyl diphosphine complex was observed, indicating that η^3-indenyl intermediate **E** loses alkyne or phosphine faster than CO.

With CO alone, a more rapid attack of CO on **3** produces η^3-indenyl intermediate **B**, which we have seen reverts to **3** about 12 times faster than it loses alkyne

(20) In contrast, we previously observed PMe_3 catalysis of CO insertion into the methyl rhenium complex $C_5H_5Re(NO)(PMe_3)(CH_3)$ to give $C_5H_5Re(NO)(PMe_3)(COCH_3)$. Casey, C. P.; Widenhoefer, R. A.; O'Connor, J. M. *J. Organomet. Chem.* **1992**, *428*, 99.

Scheme 12

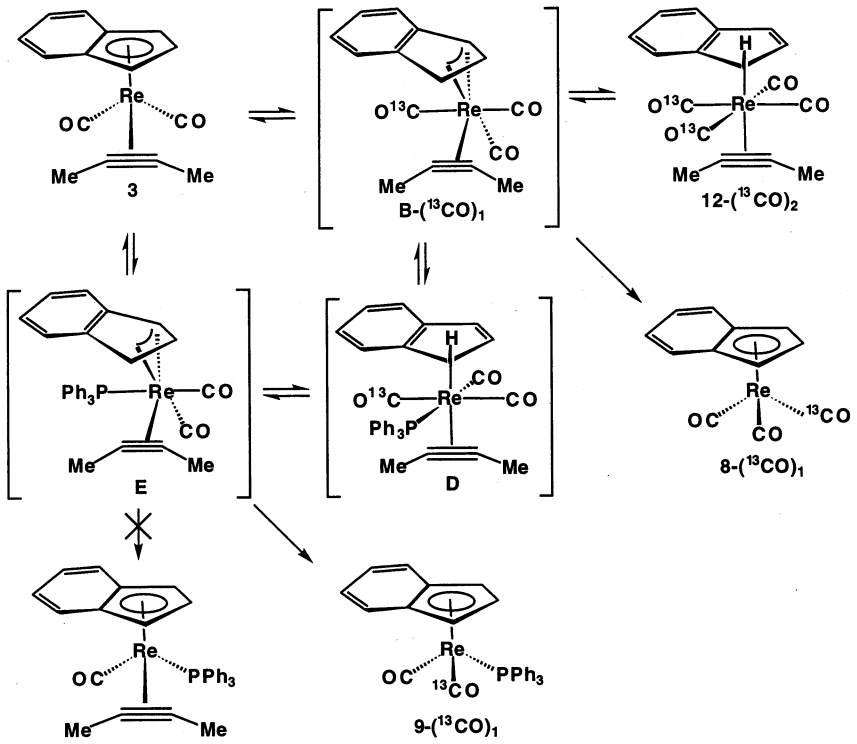

to form **8**. An explanation for the rate enhancement when both CO and PPh_3 are present is that the rapidly formed intermediate **B** is intercepted by PPh_3 to give the intermediate η^1-$C_9H_7(CO)_2(^{13}CO)(PPh_3)Re(\eta^2$-MeC≡CMe) (**D**), which then loses CO and the alkyne ligand to form **9**. This scenario explains the observations of ^{13}CO incorporation in phosphine complex **9** and of enhanced rates when both CO and PPh_3 are present.

Experimental Section

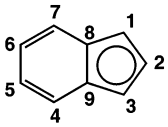

Indenyl Numbering Used in NMR Assignments. (η^5-C_9H_7)$(CO)_2$Re(η^2-MeC≡CMe) (3). Addition of excess 2-butyne (6.5 mmol) to a THF solution of **7** (250 mg, 0.58 mmol) resulted in the formation of **3** after an hour at room temperature. Flash chromatography (silica gel, 8:1 pentane−CH_2Cl_2) gave **3** (84 mg, 0.20 mmol, 35% yield) as an orange crystalline solid. ^1H NMR (500 MHz, C_6D_6): δ 6.76 (*AA′BB′*, H5,6), 6.60 (*AA′BB′*, H4,7), 5.36 (t, $J = 3$ Hz, H2), 5.23 (d, $J = 3$ Hz, H1,3), 2.05 (s, Me). $^{13}C\{^1H\}$ NMR (126 MHz, C_6D_6): δ 204.1 (CO), 125.8 (C5,6), 123.2 (C4,7), 111.5 (C8,9), 90.5(C2), 73.7 (C1,3), 67.6 (C≡), 10.9 (Me). IR (THF): 1943 (s), 1869 (vs) cm^{-1}. HRMS (EI) calcd (found) for $C_{15}H_{13}O_2Re$: *m*/*z* 412.0474 (412.0467). Anal. Calcd for $C_{15}H_{13}O_2Re$: C, 43.79; H, 3.18. Found: C, 43.57; H, 2.95.

Reaction of (η^5-C_9H_7)$(CO)_2$Re(η^2-MeC≡CMe) (3) with CO. (a) A C_6H_6 (10 mL) solution of **3** (39 mg, 95 μmol) was placed in a 6 oz. pressure reaction vessel. A star stirring bar and high stirring rates were employed to ensure equilibration of gaseous and dissolved CO. The system was pressurized with 2.1 atm of CO (15 mM). The pressure vessel was placed in a 25 °C constant-temperature bath, and 0.3 mL aliquots were periodically removed and analyzed by IR spectroscopy. The concentration of **3** was determined by integration of the carbonyl band of **3** at 1869 cm^{-1}. A plot of the ln[**3**] versus time was linear ($k_{obs} = 1.1 \times 10^{-4}$ s^{-1}, $t_{1/2} = 103$ min).

(b) A C_6D_6 (0.32 mL) solution of **3** (7.3 mg, 18 μmol) was placed under 2.9 atm ^{13}CO (205 μmol, 20 mM) in a 1.98 mL resealable NMR tube. The disappearance of the alkyne methyl resonance of **3** at δ 2.05 was followed by ^1H NMR spectroscopy at 25 °C. A plot of ln[**3**] versus time was linear ($k_{obs} = 1.3 \times 10^{-4}$ s^{-1}, $t_{1/2} = 90$ min).

(c) A C_6H_6 (10 mL) solution of **3** (10.2 mg, 25 μmol) was placed in a 30 mL stainless steel bomb containing a star stirring bar. The bomb was placed in a 25 °C water bath and pressurized with 18 atm CO (260 mM). After 10 min rapid stirring, CO and solvent were removed by rapid evaporation. The remaining solid was dissolved in C_6D_6, and ^1H NMR spectroscopy showed a 2.0:1.1 ratio of **3**:**8**, indicating $k_{obs} = 7.4 \times 10^{-4}$ s^{-1}, $t_{1/2} = 16$ min.

(d) A C_6H_6 (10 mL) solution of **3** (20 mg, 49 μmol) was placed in a 25 mL stainless steel Parr pressure bomb equipped with a high-pressure SiComp probe attached to an ASI ReactIR 1000 spectrometer. At 25 °C, the bomb was pressurized with 68 atm CO. The appearance of peaks at 1927 and 2024 cm^{-1} was monitored to determine the rate of appearance of **8**. A plot of $\ln[([\mathbf{8}]_{inf} - [\mathbf{8}])/[\mathbf{8}]_{inf}]$ versus time was linear ($k_{obs} = 9.5 \times 10^{-4}$ s^{-1}, $t_{1/2} = 12$ min). In the case of the reaction of **3** with 10 atm of CO, only **3** and **8** were observed, and both the rate of appearance of **8** ($k_{obs} = 4.16 \times 10^{-4}$ s^{-1}, $t_{1/2} = 28$ min) and the rate of disappearance of **3** ($k_{obs} = 4.13 \times 10^{-4}$ s^{-1}, $t_{1/2} = 28$ min) were measured.

At pressures between 10 and 50 atm of CO, mixtures of **3**, **8**, and **12** were seen by IR and the rate of appearance of **8** was calculated (Table 1). The IR spectra were deconvoluted into a sum of the spectra of **3**, **8**, and **12**. The molar absorptivities of the three species were used to obtain their concentrations as a function of time (Figure 3S in Supporting Information).

Determination of Percent ^{13}CO in (η^5-C_9H_7)$(CO)_2$Re-(η^2-MeC≡CMe) (3) and (η^5-C_9H_7)$Re(CO)_3$ (8). The isotopic composition of **8** obtained from reaction of **3** with ^{13}CO was analyzed by electron impact mass spectrometry. The cluster of peaks in the range *m*/*e* 384−389 due to the isotopomers of the molecular ion of **8** (37% ^{185}Re, 63% ^{187}Re, and taking into

account the 10% $^{13}C^{18}O$ concentration present in labeled ^{13}CO) was used to determine the ^{13}C labeling pattern of **8**. The observed ratio of peaks in the 384−389 range was fit as the weighted sum of the patterns calculated for **8-($^{13}CO)_1$:8-($^{13}CO)_2$:8-($^{13}CO)_3$** by minimizing the sum of the squares of the difference between calculated and observed peak intensities (Table 3, 5). Similarly the isotopic composition of **3** recovered from partial reaction of **3** with ^{13}CO was analyzed by electron impact mass spectrometry. The cluster of peaks in the range *m/e* 410−415 due to the isotopomers of the molecular ion of **3** (37% ^{185}Re, 63% ^{187}Re, and taking into account the 10% $^{13}C^{18}O$ concentration present in labeled ^{13}CO) was used to determine the ^{13}C labeling pattern of **3**. The observed ratio of peaks in the 410−415 range was fit as the weighted sum of the patterns calculated for **3-($^{13}CO)_0$:3-($^{13}CO)_1$:3-($^{13}CO)_2$** by minimizing the sum of the squares of the difference between calculated and observed peak intensities (Table 4).

(η^1-C_9H_7)Re(CO)$_4$(η^2-MeC≡CMe) (12). (a) At 77 K, a measured amount of CO was condensed into a thick walled NMR tube containing **3** (8 mg, 19 μmol) in $C_6D_5CD_3$ (0.35 mL) in order to obtain a pressure of 10 atm of CO at −15 °C. After 6 h at −15 °C, ^1H NMR spectroscopy at −50 °C showed a 6:87:6 mixture of **8** (δ 1.62 for free butyne):**3** (δ 2.10):**12** (δ 1.73). After 30 h at −15 °C, the ratio of **8**:**3**:**12** was 30:20:50.

(b) A 4:4:92 ratio of **8**:**3**:**12** was obtained as follows. A $C_6D_5CD_3$ (1.5 mL) solution of **3** (29.5 mg, 0.072 mmol) was placed in a 30 mL stainless steel pressure vessel with a stirring bar. At −10 °C, 100 atm of CO was added and the solution was stirred for 1 h at −10 °C. At −78 °C, CO was released from the pressure vessel and the toluene solution was transferred to a NMR tube cooled to −78 °C. Four freeze−pump−thaw cycles were performed to remove dissolved CO before measuring the rate of conversion of **12** to **8** and **3**. IR (C_6H_6): 1998 (s), 1946 (m) cm^{-1}. ^1H NMR (500 MHz, −65 °C, $C_6D_5CD_3$): δ 7.74 (d, J = 7 Hz, H7), 7.68 (d, J = 7 Hz, H4), 7.35 (t, J = 7 Hz, H6), 7.28 (t, J = 7 Hz, H5), 7.20 (d, J = 5 Hz, H2), 6.73 (d, J = 5 Hz, H3), 4.5 (s, H1), 1.73 (s, *Me*C≡). $^{13}C\{^1H\}$ NMR (125 MHz, −65 °C, $C_6D_5CD_3$): δ 190.5 (CO), 160.6 (C8 or C9), 152.2 (C2), 140.7 (C8 or C9), 123.7, 123.4, 123.1, 121.8, 118.7, 55.4 (Me*C*≡), 19.4 (C1), 11.1 (*Me*C≡).

Rate of Conversion of (η^1-C_9H_7)Re(CO)$_4$(η^2-MeC≡CMe) (12) to 8 and 3. A $C_6D_5CD_3$ solution (0.5 mL) of **12** (8.6 mg, 0.021 mmol) was synthesized by method b described above. The NMR tube was sealed under vacuum and placed in an NMR probe cooled to −9 °C. With a headspace of approximately 1 mL, the ending CO pressure was calculated to be between 0.9 and 1.0 atm of CO after all the CO is released from **12**. Disappearance of **12** was monitored by ^1H NMR spectroscopy by integrating the proton resonance at δ 4.5 for **12** compared to the internal standard 1,4-dioxane. The rate of disappearance of **12** was first order in **12** to over 3 half-lives (k_{obs} = 1.3 × 10^{-4} s^{-1}, $t_{1/2}$ = 87 min). The rate of disappearance of **12** was measured between −24 and 2 °C, but the reaction was monitored for only 1 half-life at 4 and −2 °C since there was significant deviation from first-order decay at longer times due to inefficient removal of CO. A 1:12 mixture of **8**:**3** was formed during the first half-life as determined by integrating the proton resonances at δ 6.58 for **8** and at δ 6.60 for **3**. The ratio of 1:12 of **8**:**3** is the average over all temperatures.

Acknowledgment. Financial support from the Department of Energy, Office of Basic Energy Sciences, is gratefully acknowledged.

Supporting Information Available: Experimental procedures for synthesis of **7**, **2**, **13**, **14**, and **16**; reactions of **2** with CO, **3** with PPh_3, ^{13}CO, CN*t*-Bu; plot of CO pressure dependence of the rate of formation of **8** from **3**; Eyring plot for disappearance of **12**; simulations of ^{13}CO incorporation into **3** and **8** at 1, 4, and 12 atm ^{13}CO; and X-ray crystal data for **2** and **3**. This material is available free of charge via the Internet at http://pubs.acs.org.

OM020884Q